

RESEARCH ARTICLE

10.1002/2016JD024892

Key Points:

- Recent extremes (the Millennium Drought and 2011 pluvial) are compared to a 500-year soil moisture reconstruction
- 2011 was likely the wettest year in the record for Coastal Queensland
- Climate projections indicate substantially increased risk of droughts \geq the magnitude of the Millennium Drought

Correspondence to:

B. I. Cook,
benjamin.i.cook@nasa.gov

Citation:

Cook, B. I., et al. (2016), The paleoclimate context and future trajectory of extreme summer hydroclimate in eastern Australia, *J. Geophys. Res. Atmos.*, 121, 12,820–12,838, doi:10.1002/2016JD024892.

Received 2 FEB 2016

Accepted 21 OCT 2016

Accepted article online 31 OCT 2016

Published online 12 NOV 2016

The paleoclimate context and future trajectory of extreme summer hydroclimate in eastern Australia

Benjamin I. Cook^{1,2}, Jonathan G. Palmer³, Edward R. Cook², Chris S. M. Turney³, Kathryn Allen⁴, Pavla Fenwick⁵, Alison O'Donnell⁶, Janice M. Lough⁷, Pauline F. Grierson⁶, Michelle Ho⁸, and Patrick J. Baker⁴
¹NASA Goddard Institute for Space Studies, New York, New York, USA, ²Lamont-Doherty Earth Observatory, Palisades, New York, USA, ³Climate Change Research Centre, School of Biological, Earth and Environmental Sciences, University of New South Wales, Sydney, New South Wales, Australia, ⁴School of Ecosystem and Forest Sciences, University of Melbourne, Richmond, Victoria, Australia, ⁵Gondwana Tree Ring Laboratory, Little River, New Zealand, ⁶Ecosystems Research Group, School of Plant Biology, University of Western Australia, Crawley, Western Australia, Australia, ⁷Australian Institute of Marine Science, Townsville, Queensland, Australia, ⁸Columbia Water Center, Columbia University, New York, New York, USA

Abstract Eastern Australia recently experienced an intense drought (Millennium Drought, 2003–2009) and record-breaking rainfall and flooding (austral summer 2010–2011). There is some limited evidence for a climate change contribution to these events, but such analyses are hampered by the paucity of information on long-term natural variability. Analyzing a new reconstruction of summer (December–January–February) Palmer Drought Severity Index (the Australia–New Zealand Drought Atlas; ANZDA, 1500–2012 Common Era), we find moisture deficits during the Millennium Drought fall within the range of the last 500 years of natural hydroclimate variability. This variability includes periods of multidecadal drought in the 1500s more persistent than any event in the historical record. However, the severity of the Millennium Drought, which was caused by autumn (March–April–May) precipitation declines, may be underestimated in the ANZDA because the reconstruction is biased toward summer and antecedent spring (September–October–November) precipitation. The pluvial in 2011, however, which was characterized by extreme summer rainfall faithfully captured by the ANZDA, is likely the wettest year in the reconstruction for Coastal Queensland. Climate projections (Representative Concentration Pathways (RCP) 8.5 scenario) suggest that eastern Australia will experience long-term drying during the 21st century. While the contribution of anthropogenic forcing to recent extremes remains an open question, these projections indicate an amplified risk of multiyear drought anomalies matching or exceeding the intensity of the Millennium Drought.

1. Introduction

At the turn of the 21st century, two extreme hydroclimate events occurred over eastern Australia in rapid succession. The first was an intense, multiyear drought referred to as the Big Dry or Millennium Drought [Cai et al., 2014; Ummenhofer et al., 2009; Verdon-Kidd and Kiem, 2009]. From the late 1990s through 2009, precipitation deficits (primarily during austral autumn) contributed to low runoff and streamflow in the Murray-Darling Basin [Kiem and Verdon-Kidd, 2010; Kirby et al., 2014; Potter et al., 2010], caused fires across Southeastern Australia [Cai et al., 2009a; Heberger, 2011] including the Black Saturday fires that claimed 173 lives and cost an estimated US\$3 billion [Cai et al., 2009a; Teague et al., 2010], and led to major economic and agricultural losses [van Dijk et al., 2013; Horridge et al., 2005; Kirby et al., 2014]. Two years after the Millennium Drought, eastern Australia went on to experience one of the wettest observed summers [Post et al., 2014; Cai and van Rensch, 2012], including record high rainfall in December of 2010 [Australian Bureau of Meteorology, 2011] and flooding in southeast Queensland and Brisbane in January 2011 that claimed 23 lives and caused US\$2.55 billion in damages [van den Honert and McAneney, 2011]. The global land precipitation anomaly that year, associated with a major La Niña event, was so large that it caused a transient drop in global sea levels [Boening et al., 2012; Fasullo et al., 2013] and a record high terrestrial carbon sink [Le Quéré et al., 2013; Poulter et al., 2014].

Extreme droughts and floods are recurring features of the climate in eastern Australia, and the historical record is replete with examples. These include the Federation (1895–1902) and World War II (1937–1945) droughts [Ummenhofer et al., 2009; Verdon-Kidd and Kiem, 2009], the 1791–1792 Settlement Drought following initial European colonization [Palmer et al., 2015; Russell, 1877], and numerous major floods

[van den Honert and McAneney, 2011; Pittock et al., 2006]. Hydroclimate in southern and eastern Australia is closely connected to three primary patterns of ocean-atmosphere variability that operate on interannual to multidecadal time scales: the El Niño–Southern Oscillation (ENSO) [Cai et al., 2011; Nicholls et al., 1996; Power et al., 1998], the Indian Ocean Dipole (IOD) [Cai et al., 2011; Ummenhofer et al., 2009, 2011], and the Interdecadal Pacific Oscillation (IPO) [Kiem and Franks, 2004; Vance et al., 2015]. Precipitation over eastern Australia is generally suppressed during warm or positive phases of these modes, with each mode exhibiting strong seasonal biases in their teleconnections over eastern Australia. ENSO has the strongest and most widespread impact in spring (September–October–November; SON) and some modest strength during winter (June–July–August; JJA) [Risbey et al., 2009]. Significant summer-season (December–January–February; DJF) ENSO teleconnections are localized primarily over Queensland and are weak and mostly nonsignificant during the autumn (March–April–May; MAM). The influence of the IOD is strongest from winter through the early spring (June–October) and is strongly amplified when a positive (negative) IOD event coincides with an El Niño (La Niña) [Risbey et al., 2009]. The IPO primarily modulates the expression of ENSO variability, especially over Queensland [Cai et al., 2010; Cai and van Rensch, 2012; Kiem et al., 2003; Kiem and Franks, 2004; Power et al., 1999], and appears to be most strongly connected with summer precipitation and drought [Palmer et al., 2015; Vance et al., 2015].

Precipitation deficits during the Millennium and other historical (Federation and World War II) droughts have been attributed to a range of phenomena. Some have pointed to a consistent absence of rainfall-enhancing negative IOD events [Ummenhofer et al., 2009, 2011]. Other analyses have suggested a more prominent role for ENSO in the Millennium Drought [van Dijk et al., 2013; Verdon-Kidd and Kiem, 2009], with additional influences from the Southern Annular Mode [Verdon-Kidd and Kiem, 2009] and the IPO [van Dijk et al., 2013]. In contrast, the extreme pluvial in 2011 was forced primarily by a large La Niña event [Cai and van Rensch, 2012; Evans and Boyer-Souchet, 2012; Lewis and Karoly, 2015], with additional contributions from negative phases of the IPO [Cai and van Rensch, 2012] and IOD [Verdon-Kidd et al., 2014] and a strong positive departure in the Southern Annular Mode [Timbal and Fawcett, 2012].

While their genesis was clearly natural, the extreme nature of these events has motivated investigations into a possible role for anthropogenic climate change. For the Millennium Drought, several studies [Cai et al., 2009b; Nicholls, 2004; Ummenhofer et al., 2009] concluded that extreme temperatures increased evaporative demand, amplifying surface drying beyond what would have occurred from the (natural) sea surface temperature (SST)-induced rainfall deficits alone. Some have concluded, however, that the high temperature anomalies were instead a response to the drought, rather than a contributing factor [Lockart et al., 2009]. Other studies suggest that the precipitation deficits themselves during the drought were possibly influenced by long-term, anthropogenically driven drying trends caused by poleward storm track shifts and the intensification and expansion of the subtropical dry zone in the Southern Hemisphere [Cai et al., 2014; Post et al., 2014; Theobald et al., 2015; Verdon-Kidd et al., 2014]. Analyses of the 2010–2011 summer have also found evidence for an anthropogenic effect on the floods and extreme rainfall from elevated SSTs [Evans and Boyer-Souchet, 2012; Hendon et al., 2014; Ummenhofer et al., 2015], although some of these results may be model dependent [Lewis and Karoly, 2015].

The Millennium Drought and 2011 pluvial were extreme, but understanding the anthropogenic climate change contribution to these events requires a more complete sampling of the range of natural climate variations than is available from the short instrumental record. This has motivated the development of several paleoclimate reconstructions to extend the climate record of eastern Australia further back in time. One of the first to specifically address the issue of the Millennium Drought was the streamflow reconstruction of Gallant and Gergis [2011] for the River Murray. They concluded that streamflow deficits during the Millennium Drought were a 1-in-1500 year event, the driest period back to 1783. This conclusion was further supported by the Gergis et al. [2012] precipitation reconstruction for Southeastern Australia, where the authors determined, with a >97% likelihood, that 1998–2008 was the driest decade in the region since initial European settlement in 1788. Two recent reconstructions, however, point to much larger natural variability in hydroclimate in centuries prior to the historical period. Ho et al. [2015] developed a rainfall reconstruction for the Murray-Darling Basin and found multiple instances of decadal length dry and wet periods over the last two millennia that exceeded any event in the instrumental record. Vance et al. [2015], in a millennial length IPO reconstruction from the Law Dome ice core, similarly identified periods of persistent drought in eastern Australia over the past millennium, including exceptional aridity during the 1100s. Notably, reconstructions of

precipitation over southwestern Australia suggest that some of these periods of prolonged aridity may have even extended across the entire southern half of the continent [Cullen and Grierson, 2009].

There are thus still considerable uncertainties regarding how the Millennium Drought and 2011 pluvial compare to natural hydroclimate variations over recent centuries, especially in a broader spatiotemporal context. Here we build on previous work by conducting a new analysis of the Australia-New Zealand Drought Atlas (ANZDA), an annually and spatially resolved proxy (tree rings and corals) reconstruction of hydroclimate variability for eastern Australia, Tasmania, and New Zealand [Palmer *et al.*, 2015]. Combined with climate model projections from Phase 5 of the Coupled Model Intercomparison Project (CMIP5) [Taylor *et al.*, 2012], we investigate the past context and future trajectory of extreme hydroclimate events in eastern Australia. Specifically, we focus on two research questions: (1) How do the Millennium Drought and 2011 pluvial (wet spell) compare to the full range of drought variability over the last 500 years, as represented in the ANZDA? and (2) How will the probability of similar events shifts with climate change over the 21st century?

2. Materials and Methods

2.1. The Australia-New Zealand Drought Atlas (ANZDA)

The ANZDA [Palmer *et al.*, 2015] is a gridded (0.5° spatial resolution), annually resolved reconstruction of austral summer self-calibrating Palmer Drought Severity Index (PDSI) [Palmer, 1965]. The year is centered on January so that, for example, values for 2011 represent the average of December 2010, January 2011, and February 2011. PDSI is a normalized indicator of drought, using a soil moisture bucket model to simultaneously track changes in moisture supply (precipitation) and demand (evapotranspiration) from month to month. PDSI integrates changes in the surface moisture balance over a time scale of approximately 12 months [Guttman, 1998] and compares well with more sophisticated soil moisture models [e.g., Cook *et al.*, 2015; Williams *et al.*, 2015]. The DJF PDSI used in our analysis of Australian hydroclimate thus differs from other drought indicators (e.g., precipitation and streamflow) in terms of (1) the aspect of the hydrologic cycle it most closely represents (soil moisture) and (2) its inherent seasonality (likely biased toward spring and summer, while still incorporating climate information from previous seasons). It is expected, therefore, that results and conclusions drawn from analyses of PDSI may differ from studies targeting other hydroclimatic variables [e.g., Gallant and Gergis, 2011; Gergis *et al.*, 2012]. Positive values of PDSI indicate wetter than normal conditions (pluvials), while negative values indicate drier than normal conditions (droughts). PDSI is widely used as a paleoclimate reconstruction target [Cook *et al.*, 2004, 2010; Smerdon *et al.*, 2015] and in observational [e.g., van der Schrier *et al.*, 2013] and model-based [e.g., Cook *et al.*, 2014] analyses of drought dynamics.

While different from what may be considered more standard hydroclimate variables (e.g., precipitation anomalies and streamflow deficits), summer-season PDSI is a valuable drought indicator in many regions, including eastern Australia. PDSI integrates climate across multiple months and seasons, providing a longer-term view of moisture deficits and surpluses than can be derived from monthly precipitation anomalies alone, and incorporates information on both moisture supply and demand, representing a more complete picture of the surface moisture balance. This is especially critical for analyzing climate change impacts on drought, which are expected to arise from shifts in both precipitation and evaporative demand [e.g., Cook *et al.*, 2014, 2015; Scheff and Frierson, 2013; Williams *et al.*, 2015]. More specifically for Southeastern Australia, summer PDSI is an indicator of initial soil moisture conditions for the winter cropping season. The impacts of insufficient precipitation during the growing season and at the start of the cropping season are exacerbated by a preceding dry summer, especially in areas that practice minimal tillage farming and sow before the autumn breaking rains [Pook *et al.*, 2006]. Fire risks across large areas of arid and semiarid Australia are also influenced by low soil moisture levels that increase the ability for fuel to burn and can also temporarily increase litter fall from vegetation, further increasing fuel loads [Bradstock, 2010]. Because of its warm season bias, summer PDSI can also be a good proxy for extreme rainfall and flooding, especially for summer-dominated rainfall regions (e.g., northern Australia) where these events can be devastating [Holmes, 2012].

The ANZDA reconstruction (1500–2012) is based on a network of 176 drought-sensitive tree-ring chronologies and one coral luminescence proxy series. PDSI values in the ANZDA from 1500 to 1975 are derived from the proxy network and merged with the underlying instrumental data set [van der Schrier *et al.*, 2013] from 1976 to 2012. The leading principal component in the ANZDA explains >50% of the underlying variance and is strongly correlated with the IPO [Palmer *et al.*, 2015]. The reconstruction validates well over

eastern Australia and identifies droughts that are independently corroborated in other reconstructions and historical documents. Full details, including complete calibration and validation information, can be found in Palmer *et al.* [2015].

2.2. CMIP5 Simulations

To investigate climate change impacts on drought, we use PDSI calculated from CMIP5 model projections of the 21st century (available from http://www.ideo.columbia.edu/~jsmerdon/2014_clidyn_cooketal_supplement.html, Cook *et al.* [2014]). These projections cover the time interval 1901–2099, using the historical (1850–2005) and RCP 8.5 (2006–2099; business-as-usual, high greenhouse gas emissions) forcing scenarios. This ensemble includes projections from 15 models, several with multiple ensemble-members, for a total of 34 individual simulations. These model PDSI calculations use the physically based Penman-Monteith formulation for potential evapotranspiration (PET) [Smerdon *et al.*, 2015], incorporating model trends in temperature, humidity, and net radiation (the PDSI target field [van der Schrier *et al.*, 2013] for the ANZDA reconstruction also used Penman-Monteith). Because the Penman-Monteith formulation is a more physically based approximation of PET, it avoids the limitations of more simple PET methods (e.g., Thornthwaite) that overestimate temperature and PET-forced drought trends [e.g., Hoerling *et al.*, 2012]. We analyze DJF average PDSI from these projections for consistency with the ANZDA. Further details on these drought projections and PDSI calculations can be found in Cook *et al.* [2014], including global PDSI projections for each individual model.

2.3. Analyses

Prior to any analysis, PDSI data from the CMIP5 simulations and ANZDA at each grid point were recentered to a mean of zero over the 20th century (1901–2000). This ensures the same baseline average conditions for comparing drought variability across the reconstruction and model simulations. To identify regions for time series analysis, we first conducted a principal component analysis (PCA) on the continental Australia portion of the ANZDA, retaining and rotating the first three modes using varimax rotation. The resulting three rotated modes account for 68.5% of the underlying variance with three primary centers of action (Figure 1). The first is over southeast Australia and the Murray-Darling Basin (“Southeastern Australia”; 138–154°E, 28–39.5°S). The second mode is focused to the west of the Great Dividing Range in Queensland (“Western Queensland”; 138–145°E, 18–28°S). The third and final principal component projects most strongly along the coast of northeastern Australia (“Coastal Queensland”; 145–154°E, 18–28°S). Using the PCA analysis for guidance, we then spatially averaged PDSI over these regions from the ANZDA and CMIP5 model simulations to generate time series for analysis. Uncertainties in our reconstructed regional drought series are calculated as the 90th percentile prediction intervals, estimated from a linear regression between the tree ring and instrumental PDSI from 1902 to 1929 (the independent validation interval used in the ANZDA reconstruction). To quantify drought risk, we empirically fit kernel densities (cumulative distribution functions) to these regional average PDSI distributions in the ANZDA and CMIP5 simulations. Comparisons between the fully reconstructed (1500–1975) and instrumental (1902–2012) PDSI showed no significant differences ($p > 0.05$) in either median PDSI (Wilcoxon rank-sum test) or dispersion (Ansari-Bradley test). To provide context for recent extreme hydroclimate events, we highlight, from the ANZDA record, previous extreme drought and pluvial years.

To compare and evaluate our results within the context of seasonal precipitation variability, we conducted two sets of comparisons between PDSI and precipitation. First, we calculated Spearman’s rank correlations (1902–1929) between the PDSI (tree ring reconstructed and instrumental) and single and cumulative season precipitation from the CRU 3.21 climate grids [Harris *et al.*, 2014]. These are the same precipitation data used in the construction of the instrumental PDSI [van der Schrier *et al.*, 2013] targeted in the ANZDA reconstruction. Second, we compare our reconstructed PDSI time series from Southeastern Australia to the historical precipitation reconstruction of Ashcroft *et al.* [2014]. This regional precipitation data set consists of seasonal, standardized precipitation anomalies for 1860–2012, constructed from homogenized historical precipitation records distributed across a region (136–154°E and 26–40°S) approximately equivalent to our defined Southeastern Australia region. For the Ashcroft *et al.* [2014] comparison, we calculate Spearman’s rank correlations between seasonal precipitation and reconstructed PDSI for three intervals (1860–1901, 1902–1929, and 1930–1975) and compare anomalies during the major multiyear historical drought events (Federation, World War II, and Millennium). As with the PDSI from the ANZDA and CMIP5 simulations, we recentered these seasonal precipitation anomalies to a zero 20th century mean prior to any analyses.

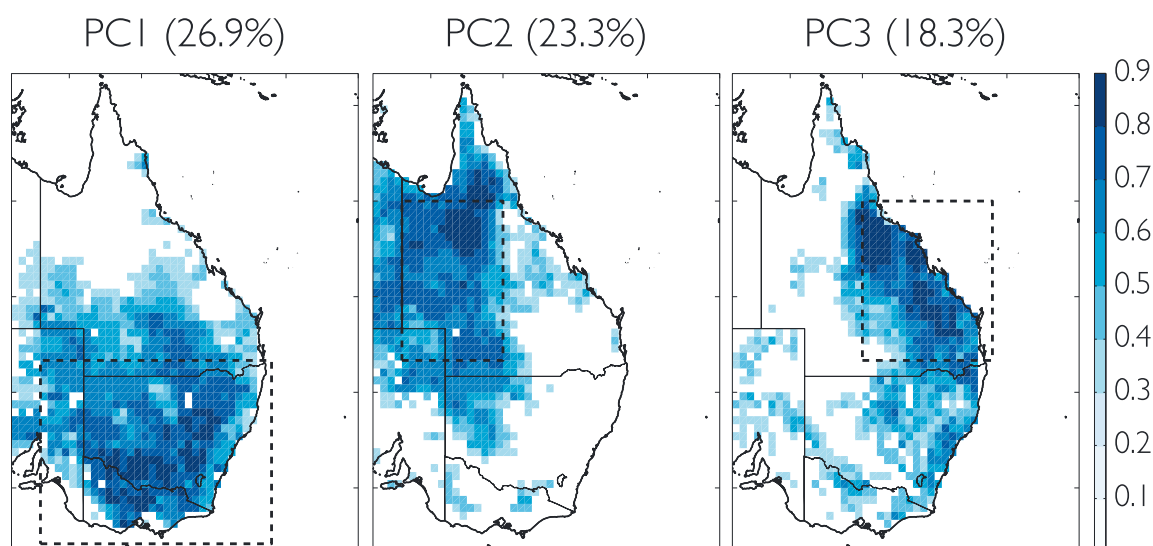


Figure 1. Loadings for the first three varimax rotated principal components for the eastern Australia portion of the ANZDA. Percentages in the titles indicate the proportion of variance explained by each mode. Dashed boxes indicate our main regions of study over which we generate the regional average PDSI time series from the ANZDA. These correspond to the major centers of loading of the three principal components: Southeastern Australia (PC1; 138°–154°E, 28°–39.5°S), Western Queensland (PC2; 138°–145°E, 18°–28°S), and Coastal Queensland (PC3; 145°–154°E, 18°–28°S).

Aside from analyzing single-year droughts and pluvials in the reconstruction and CMIP5 simulations, we also target analogues for the Millennium Drought. We define our Millennium Drought analogues as 7-year running mean PDSI (in either the reconstruction or model ensemble) with a magnitude equal to or drier than the 7-year mean for the Millennium Drought (2003–2009). We acknowledge that this ignores situations where two dry 7-year analogues may overlap or occur as part of the same persistent drought event. However, we use this as the most straightforward method for determining how the Millennium Drought compares to equivalent periods in the ANZDA, and how the risk of similar events may change under increased greenhouse gas forcing.

3. Results

3.1. The Millennium Drought and 2011 Pluvial

PDSI is primarily an indicator of soil moisture variability, integrated over multiple seasons. It is expected, then, that PDSI may record drought differently compared to variables that track other parts of the hydrologic cycle, such as precipitation or streamflow. Most studies based on precipitation deficits [e.g., *Ummenhofer et al.*, 2009] define the Millennium Drought from the mid-1990s to 2008 or 2009. In the ANZDA, average PDSI over all three of our study regions in 2002 is -0.16 , only slightly below normal. The following year is the first major and widespread year of drought in the data set, with three-region average PDSI $= -2.13$. Given this, we therefore define the Millennium Drought from 2003 to 2009, acknowledging that analyses of other hydroclimatic variables may lead to different results and interpretations.

Drought conditions were most intense and widespread in the ANZDA in the first year (2003) of the Millennium Drought (Figure 2), covering most of eastern Australia from Tasmania to the Cape York Peninsula. By 2008 and 2009, conditions had either ameliorated or recovered across most of the continent except for some intensification in the south. The year 2011 was exceptionally wet over nearly all of eastern Australia (Figure 2), with grid cell values of PDSI in excess of $+5$ in all three regions. During 2011, values of area averaged PDSI were positive enough that all three regions qualified as “very wet” by the standard PDSI scaling definitions (<http://drought.unl.edu/Planning/Monitoring/ComparisonofIndicesIntro/PDSI.aspx>) (Western Queensland PDSI $= +4.32$, Coastal Queensland PDSI $= +5.24$, and Southeastern Australia PDSI $= +3.82$).

3.2. Precipitation Seasonality in the ANZDA

Instrumental and reconstructed summer-season PDSI are mostly positively and significantly (one-sided test, $p \leq 0.05$) correlated with instrumental precipitation (Figure 3). The strongest single-season precipitation correlations are summer and antecedent spring, with weaker but mostly still significant correlations with antecedent winter and autumn. Both instrumental and reconstructed PDSI show small negative correlations with preceding single-season autumn precipitation for Southeastern Australia. The presence of the negative

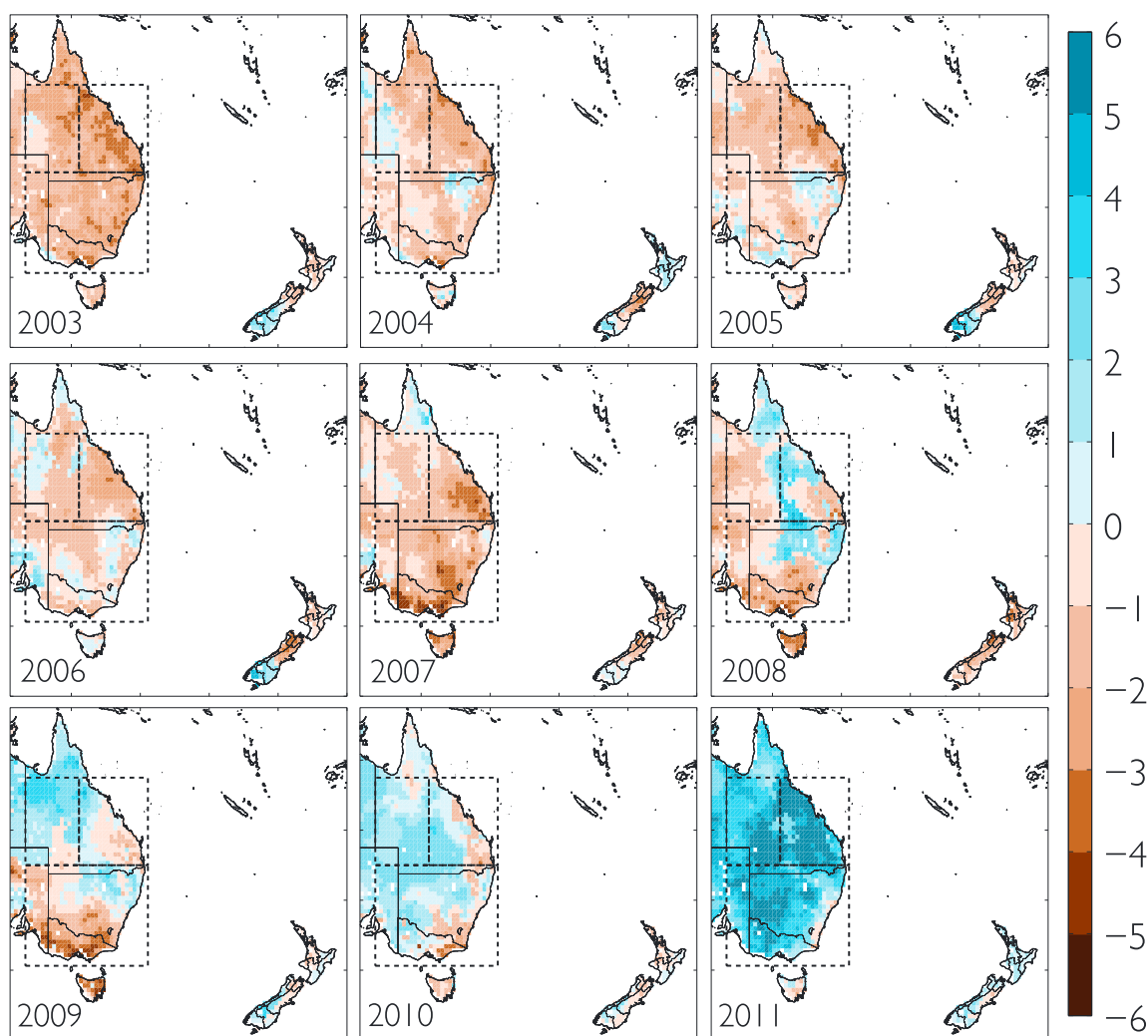


Figure 2. Austral summer (December–January–February; DJF) PDSI from the ANZDA during the Millennium Drought (2003–2009) and 2011 pluvial in eastern Australia. Dashed boxes outline our three primary regions of analysis identified in Figure 1.

correlation in the instrumental PDSI comparison indicates this is not an artifact of the reconstruction process and thus may reflect some biases or noise over this relatively short period (28 years) in the instrumental record. The cumulative seasonal correlation plots clearly show the important secondary influence of these previous seasons on the summer PDSI. In nearly all cases, instrumental PDSI correlations with cumulative precipitation from multiple seasons (e.g., SON+DJF) are stronger than any single season, with the largest increase in correlation occurring when SON is combined with DJF. Seasonal correlation patterns for the reconstructed PDSI are similar (and $\geq +0.6$ for Coastal Queensland and Southeastern Australia), although the winter and autumn signals in the reconstructed PDSI are weaker in both the single and cumulative season cases. This likely reflects some additional biases in the underlying proxies toward spring and summer (beyond those embedded in the PDSI calculation), or potential non-PDSI related variability in the proxies themselves.

The reconstructed PDSI is also positively and significantly correlated with the *Ashcroft et al.* [2014] historical precipitation reconstruction over Southeastern Australia (Figure 4). Correlations with cumulative season precipitation are similar, or even slightly higher, during the ANZDA verification interval (1902–1929) compared to the later calibration period (1930–1975), though they are substantially lower during the late 19th century (1860–1901). Proxy availability in the reconstruction, however, is nearly uniform over the entire period, suggesting the decreased correlation strength may instead reflect changes in the earliest precipitation records used in the historical precipitation reconstruction. Indeed, the network of stations in the *Ashcroft et al.* [2014] reconstruction for the late 19th century increases from less than 20 in 1860 to over 40 in 1900 [*Gergis and Ashcroft*, 2013, Figure 3]. Regardless, correlations with the ANZDA are mostly significant in all seasons for

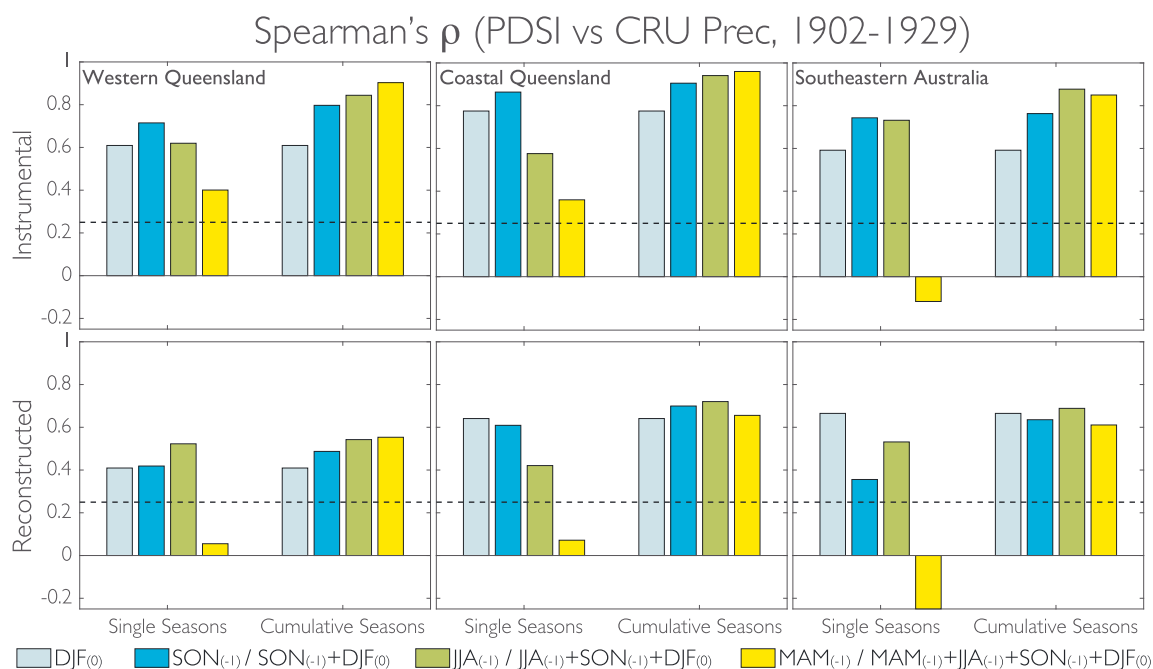


Figure 3. Correlations (Spearman's rank) between single and cumulative season CRU precipitation and instrumental (top row) and reconstructed (bottom row) regional average summer (December-January-February; DJF) PDSI from the ANZDA. Seasonal subscripts indicate correlations with concurrent (0) or preceding (−1) seasons. Dashed black lines represent the threshold for significance ($p \leq 0.05$, one-sided test for positive correlation).

all intervals, with the strongest relationship between summer PDSI and cumulative spring and summer precipitation, a result consistent with the previous CRU precipitation analysis. Combined with the instrumental analysis, these results demonstrate the ability of the reconstructed PDSI to capture a substantial fraction of the cumulative season precipitation variability in all three regions.

Differences in the magnitude of the precipitation and PDSI anomalies are apparent across the three major multiyear historical era droughts (Figure 5). Autumn precipitation deficits were the main driver of the Millennium Drought [e.g., *Timbal and Fawcett*, 2013] with secondary contributions from more modest deficits in the winter and spring. This is confirmed in the *Ashcroft et al.* [2014] reconstruction, which shows autumn precipitation deficits during the Millennium Drought were the largest single-season precipitation anomalies across these three events. Summer season PDSI in the ANZDA, however, was slightly drier during the World War II drought compared to the Millennium Drought, which can likely be explained in terms of the precipitation seasonality in the ANZDA. As noted, the sensitivity of the summer season PDSI to autumn precipitation is weaker than for the other three seasons, which suggests that the ANZDA may underestimate the magnitude of the

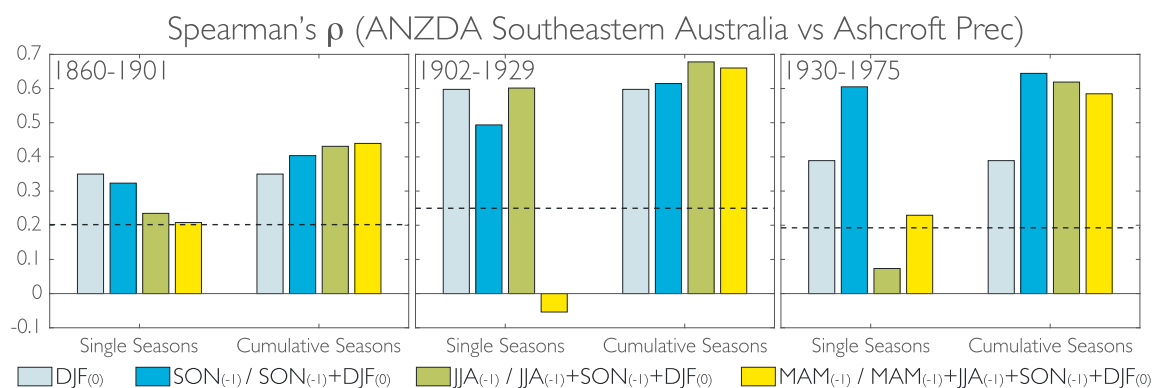


Figure 4. Correlations (Spearman's rank) between the Southeastern Australia reconstructed ANZDA summer (December-January-February; DJF) PDSI and the single and cumulative season historical precipitation from the *Ashcroft et al.* [2014] reconstruction. Seasonal subscripts indicate correlations with concurrent (0) or preceding (−1) seasons. Dashed black lines represent the threshold for significance ($p \leq 0.05$, one-sided test for positive correlation).

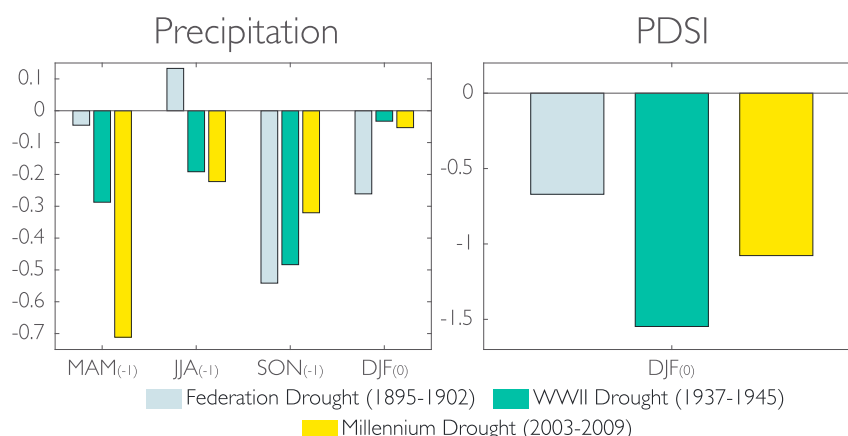


Figure 5. Seasonal precipitation [Ashcroft *et al.*, 2014] and ANZDA summer (December-January-February; DJF) PDSI anomalies for the three major multiyear historical droughts in Southeastern Australia: the Federation Drought, World War II Drought, and Millennium Drought. PDSI anomalies are based on the standard PDSI scaling, while units for precipitation are standardized anomalies. Subscripts indicate composites of concurrent (0) or antecedent (−1) seasonal anomalies in the multiyear average (relative to the summer).

Millennium Drought. The World War II drought, however, was forced by the single largest SON precipitation deficit across the three events, a season that is strongly correlated with summer season PDSI and an event that the ANZDA is well suited to capture. This again highlights the seasonal biases in the ANZDA summer PDSI and indicates the need for caution when interpreting and drawing conclusions about hydroclimate events expressed across different drought indicators and variables.

3.3. Hydroclimate Variability Over the Last 500 Years

The last 500 years of hydroclimate variability are shown for our three regions combined (Figure 6) and individually (Figure 7). Over the ANZDA verification interval (1902–1929), the instrumental and reconstructed PDSI

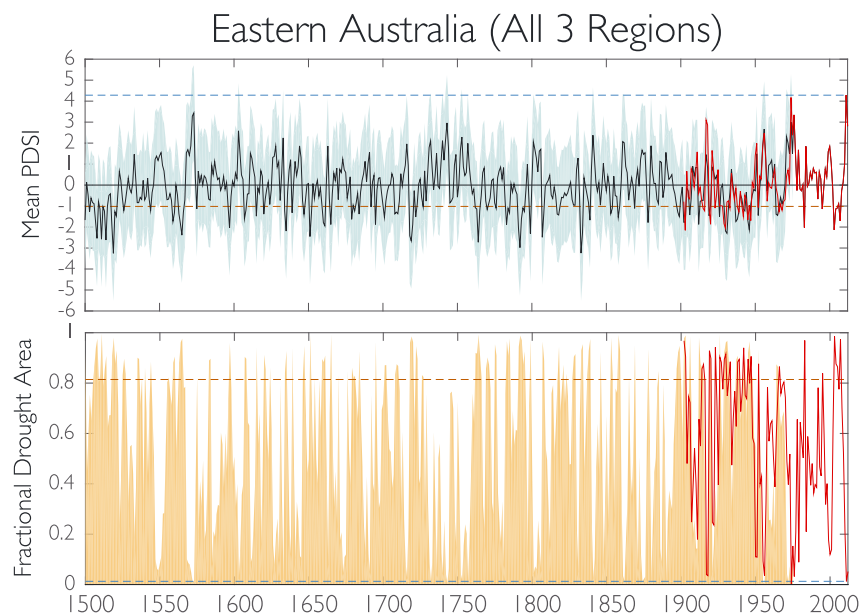


Figure 6. Regional average summer (December-January-February; DJF) (top) PDSI and (bottom) fractional drought area ($PDSI < 0$) from the ANZDA, calculated for our three eastern Australia regions combined: Western Queensland, Coastal Queensland, and Southeastern Australia. Uncertainties in the reconstruction are shown in blue-grey shading, estimated as the 90th percentile prediction intervals from a linear regression between the tree ring and instrumental PDSI time series over 1902–1929 (the independent reconstruction verification interval). Solid red lines are regional average PDSI and drought area calculated from the instrumental PDSI. Dashed brown lines are the multiyear mean PDSI and drought area associated with the Millennium Drought (2003–2009). Dashed blue lines are the same but for the 2011 pluvial.

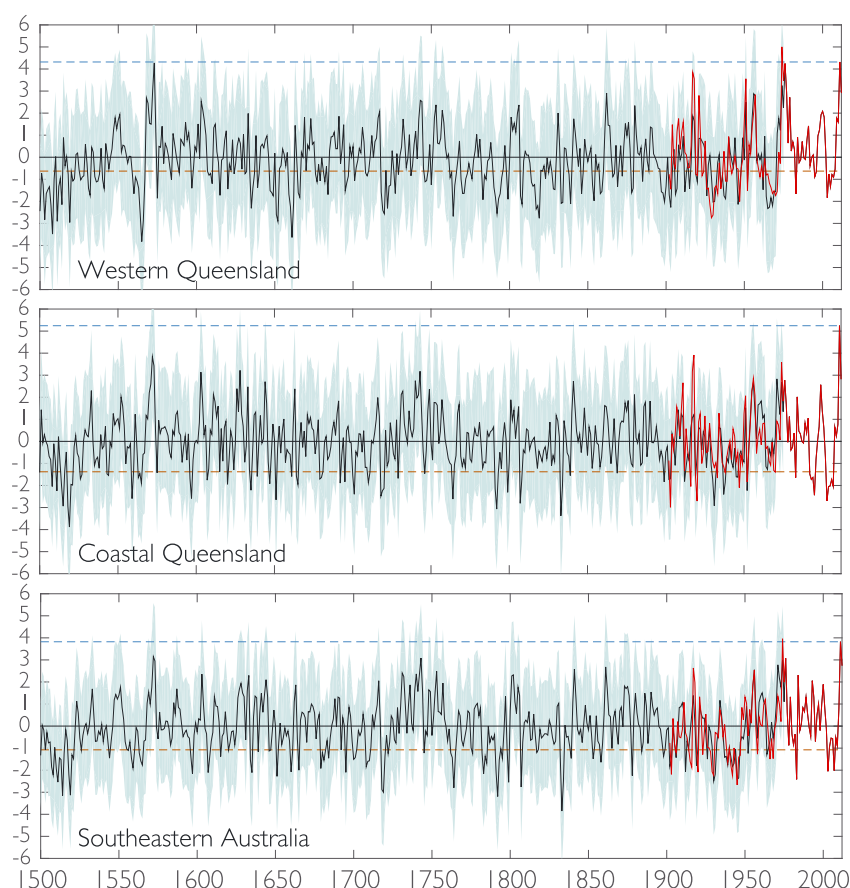


Figure 7. Regional average summer (December–January–February; DJF) PDSI for our three eastern Australia regions: Western Queensland, Coastal Queensland, and Southeastern Australia. Uncertainties in the reconstruction are shown in blue-grey shading, estimated as the 90th percentile prediction intervals from a linear regression between the tree ring and instrumental PDSI time series over 1902–1929 (the independent reconstruction verification interval). Solid red lines are regional average PDSI and drought area calculated from the instrumental PDSI. Dashed brown lines are the multiyear mean PDSI and drought area associated with the Millennium Drought (2003–2009). Dashed blue lines are the same but for the 2011 pluvial.

correlate significantly (Spearman's rank correlations): $\rho = 0.587$ in Western Queensland, $\rho = 0.707$ in Coastal Queensland, $\rho = 0.510$ in Southeastern Australia, and $\rho = 0.641$ for all three regions combined. This level of skill is comparable to the southeast Australia precipitation reconstruction of *Gergis et al.* [2012] (verification period correlations between 0.41 and 0.70; their Tables 4 and 5) and the streamflow reconstruction of *Gallant and Gergis* [2011] (verification period correlations between 0.46 and 0.70; their Table 4). The interannual variability in drought area (PDSI < 0; Figure 6, bottom) is high, a pattern exemplified by the recent extreme events that are the focus of this study. The multiyear average drought area for the Millennium Drought (2003–2009; red dashed line) covered 81.4% of eastern Australia, with 2003 appearing as the driest year of this drought in terms of PDSI anomaly (−2.13) and among the top ten most widespread (98.5% drought area) drought years since at least 1500 Common Era (C.E.). Similarly, exceptional wetness was widespread across eastern Australia in 2011 (blue dashed line), with only 1.3% of the area in drought during this time. The regional ANZDA time series (Figure 7) clearly identify major historical droughts that occurred outside the reconstruction calibration interval (1930–1975), including the well-documented Federation Drought (1895–1902) and the Settlement Drought of 1791–1792. Other periods of enhanced aridity in the ANZDA are corroborated by other reconstructions [*Ho et al.*, 2015], including the early 1500s, late 1700s, and 1820s to 1840s. From a summer PDSI perspective, 2011 (dashed blue line, Figures 6 and 7) stands out as exceptionally wet. Multiyear mean PDSI during the Millennium Drought (dashed brown line, Figures 6 and 7), however, appears to fall well within the range of variability (and uncertainties) in the reconstruction.

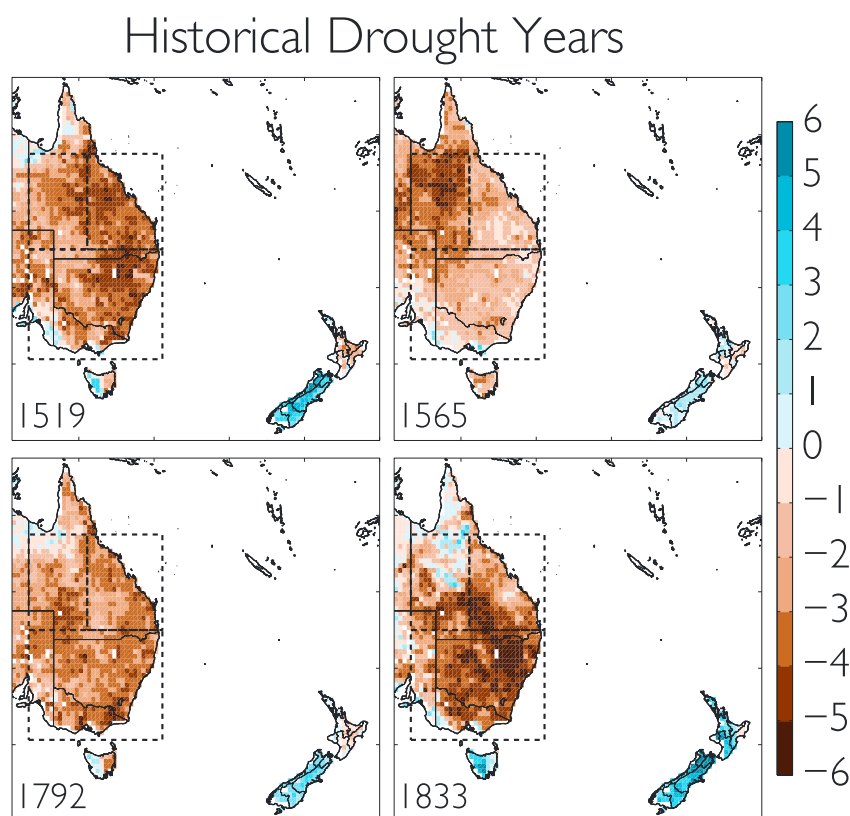


Figure 8. Reconstructed summer (December–January–February; DJF) PDSI from selected extreme single drought years in the ANZDA. 1519 was the driest year in Coastal Queensland (top five driest in Western Queensland and Southeastern Australia), 1565 was the driest in Western Queensland, and 1833 was the driest year in Southeastern Australia (top five driest in Coastal Queensland). The drought in 1792 occurred soon after the initial European colonization of the continent. This extreme year ranked among the top five driest years in Southeastern Australia and Coastal Queensland.

Nominally, the driest year of the Millennium Drought in each region was 2003, and the driest single years in the record were 1519 (Coastal Queensland), 1565 (Western Queensland), and 1833 (Southeastern Australia) (Figure 8). The Settlement Drought (1792) was also notable and appears as a significant event in the ANZDA, ranking in the top five driest for Southeastern Australia and Coastal Queensland. This drought had major impacts in New South Wales, causing a partial failure of the wheat harvest and threatening the water supply in Sydney [Russell, 1877], and occurred in conjunction with a large El Niño [Li *et al.*, 2013] that also caused significant drought in South Asia [Grove, 1998] during the same year (note, though, some overlap in the proxies used in the ANZDA and the Li *et al.* [2013] ENSO reconstruction).

The 7-year mean PDSI for the Millennium Drought (2003–2009) does not rank as exceptionally dry in any region when compared to all other possible 7-year running mean PDSI values in the ANZDA. As noted previously, this is likely due, at least in part, to the fact that the Millennium Drought was primarily driven by precipitation deficits during the autumn, the season with the weakest signal in the ANZDA. In all three regions, the driest 7-year running mean PDSI occurred during the 16th century (Figure 9). This includes two extremely dry 7-year periods in the early 1500s that were part of a persistent, multidecadal drought event in all three regions. To quantify this event, we use a simple criteria (described in Coats *et al.* [2013, 2015]) where multiyear drought events are defined as starting with two consecutive dry years ($\text{PDSI} < 0$) and ending with two consecutive wet years ($\text{PDSI} \geq 0$) (“two-start two-end”; 2S2E). By this metric, the early 1500s drought is the longest in all three regions: 1500–1522 (23 years) in Western Queensland, 1500–1527 (28 years) in Coastal Queensland, and 1500–1522 (23 years) in Southeastern Australia.

Compared to the ANZDA reconstructed PDSI (1500–1975), 2011 is the wettest single year for all three regions. When comparing across the instrumental PDSI data set (1902–2012), however, 1974 is nominally the wettest in both Western Queensland and Southeastern Australia, while 2011 remains the wettest in

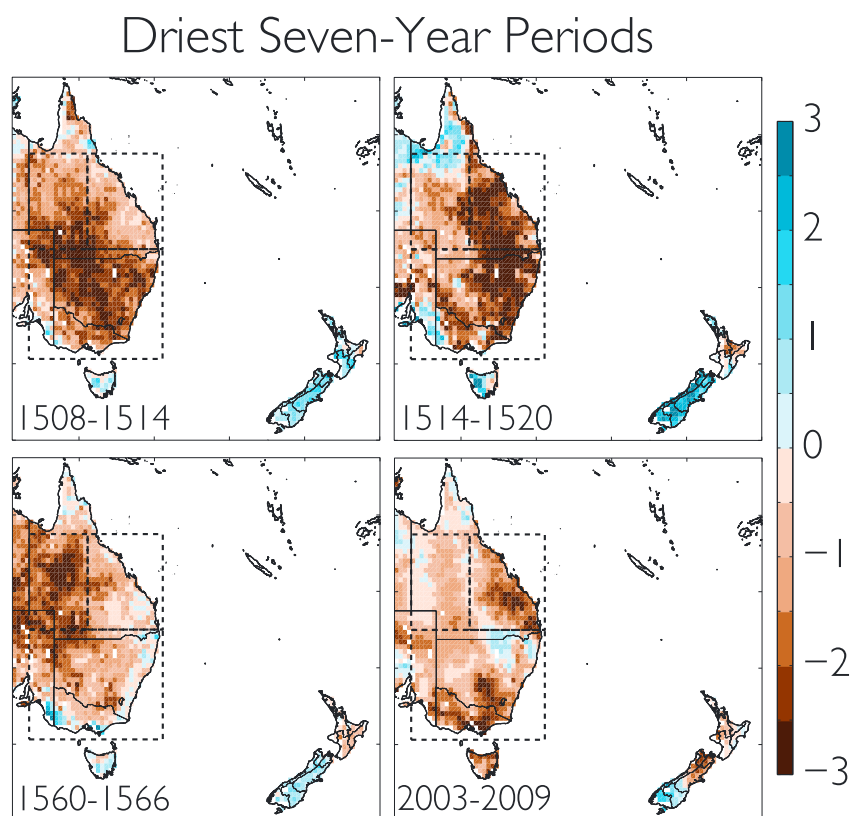


Figure 9. Reconstructed (pre-1975) and instrumental (post-1975) summer (December–January–February; DJF) PDSI for the Millennium Drought (2003–2009) and the driest 7-year running mean PDSI periods in each region: Southeastern Australia (1508–1514), Coastal Queensland (1514–1520), and Western Queensland (1560–1566). Note the reduced range on the colorbar compared to Figure 8.

Coastal Queensland. Other major wet years in the ANZDA (Figure 10) include 1572 and 1573, both major La Niña events in the reconstruction of *Li et al.* [2013], ranking among the top six wettest years in all three regions. Despite differences in ranking for 1974 between the instrumental and reconstructed PDSI, reconstructed PDSI for 1974 and 1976 are both still exceptionally wet in Western Queensland and Southeastern Australia, ranking among the top five wettest years for both regions. These relatively wet conditions in the 1970s coincided with multiyear flooding of Lake Eyre [Allan, 1985] and may have contributed, at least in part, to the overallocation of water resources in subsequent decades [Quiggin, 2001; Wei et al., 2011; Young and McColl, 2003].

For most of these events in the ANZDA it is difficult to assign exact ranks with statistical confidence because of the significant overlap in the error estimates (i.e., shaded blue regions, Figures 6 and 7). In light of this, rankings of most dry and wet years in the ANZDA are best interpreted more generally, rather than in terms of their exact position relative to other years. However, the most extreme wet years in the instrumental and reconstructed PDSI (1974 in Western Queensland and Southeastern Australia, and 2011 in Coastal Queensland) do stand apart, even when accounting for uncertainty in the reconstruction. We calculate for how many years instrumental PDSI values for 1974 in Western Queensland and Southeastern Australia and 2011 in Coastal Queensland fall outside the upper prediction interval for the reconstruction (1500–1975). This represents, effectively, a one-tailed test ($p \leq 0.05$) of the null hypothesis that these years are *not* the wettest in the record. PDSI in 1974 falls outside the confidence interval in 432 of 476 reconstructed years (90.8% of years) for Southeastern Australia and 457 of 476 reconstructed years (96.0% of years) in Western Queensland, making it likely that 1974 was the wettest event in these regions. For Coastal Queensland, 2011 stands out as even more extreme. PDSI values for 2011 in this region fall outside the upper prediction interval in 464 of the 476 reconstructed years (> 97% of years). This translates to only 12 years in the entire reconstruction that may have been wetter than 2011 in Coastal Queensland, given the uncertainties in the reconstruction. From this, we conclude that 2011 was likely the wettest summer in Coastal Queensland back to 1500 C.E.

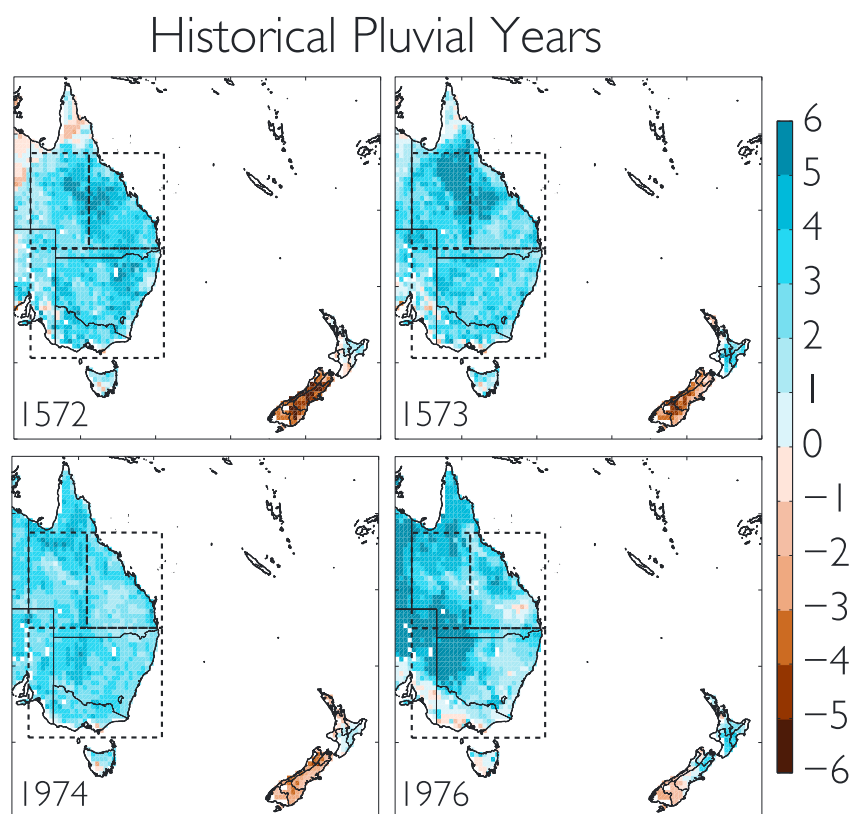


Figure 10. Reconstructed (pre-1975) and instrumental (post-1975) summer (December-January-February; DJF) PDSI for extreme wet years in the ANZDA: 1572 (top 5 wettest in Southeastern Australia and Western Queensland), 1573 (top 10 in all three regions), 1974 (top 5 in Western Queensland and Southeastern Australia), and 1976 (top 10 in all three regions).

3.4. CMIP5 PDSI Projections

For 1902–1975, we compared the cumulative probability distributions of instrumental PDSI, reconstructed PDSI, and PDSI calculated from the multimodel CMIP5 ensemble (Figure 11, left column). For all comparisons (observed versus reconstructed PDSI, observed versus CMIP5 PDSI, reconstructed versus CMIP5 PDSI), we found no significant differences in the underlying distributions (two-sided Kolmogorov-Smirnov test, $p > 0.05$) indicating, at least in aggregate, that the CMIP5 ensemble adequately captures the observed and reconstructed hydroclimate variability over this interval. We also compared the frequency (Figure 11, middle column) of major drought ($\text{PDSI} \leq -1$) and pluvial years ($\text{PDSI} \geq +1$) for each individual model simulation (box and whisker plots) and the instrumental (red dots) and reconstructed (green dots) PDSI. Both observed and reconstructed drought and pluvial frequencies fall within the range of the CMIP5 ensemble, with largest differences in Western Queensland where the models and reconstructed PDSI diverge most strongly from the observations. It is difficult to know, however, whether these disagreements arise from biases related to the fewer number of years in the observed and reconstructed PDSI relative to the large CMIP5 ensemble. Finally, we compare the frequencies of droughts of different length between the models and reconstruction using the 2S2E criterion discussed previously (Figure 11, right column). To best sample the longest drought events, here we calculate the distributions for the full ANZDA (1500–2012) and from the CMIP5 ensemble for 1901–2012 (i.e., before the major greenhouse gas forced signal in these simulations emerges). Overall, the models generally simulate fewer long-term droughts than the ANZDA reconstruction, especially in Western Queensland and Southeastern Australia.

For the latter half of the 21st century (2050–2099, RCP 8.5 scenario), the general model consensus over eastern Australia is for a shift toward more negative mean PDSI values, indicative of drier average conditions relative to the 20th century (Figure 12). Cross-model consistency is generally larger for Southeastern Australia, with only a subset of models (CanESM2, CCSM4, CNRM-CM5, MIROC5, and NorESM1-M) suggesting a tendency for

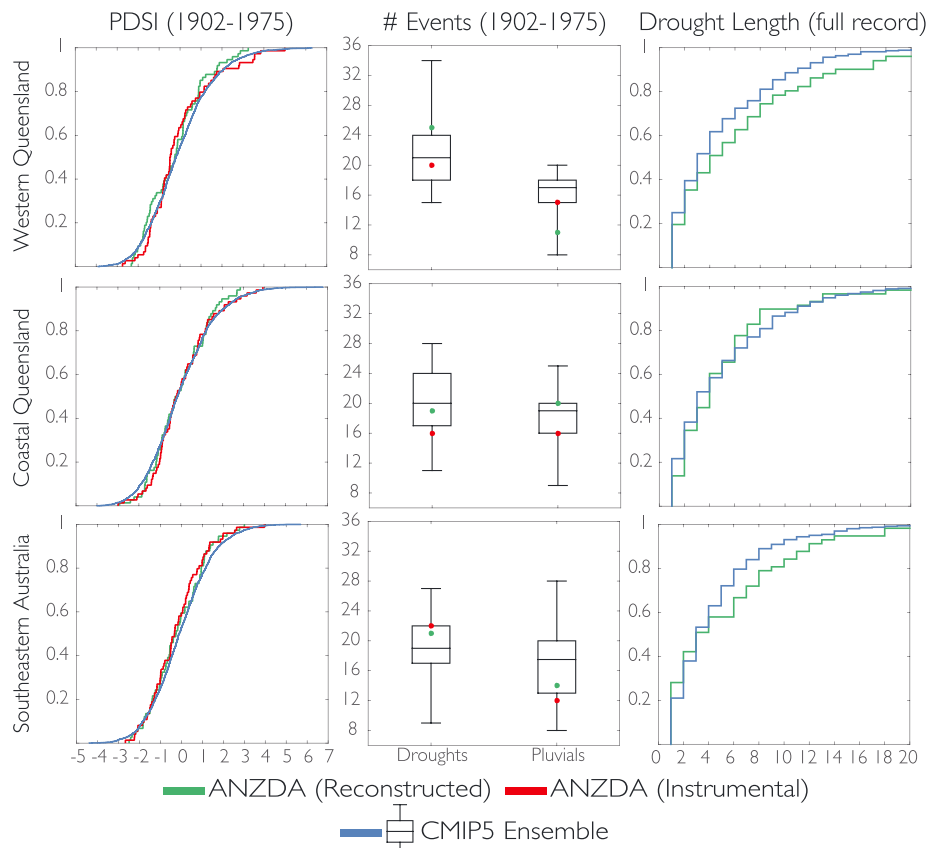


Figure 11. (left column) Empirical 20th century (1902–1975) cumulative distribution functions from the ANZDA (tree ring reconstructed and instrumental) and CMIP5 ensemble. For the ANZDA, $n = 74$ (one realization of the historical record in the observations); for CMIP5, $n = 3400$ (34 different ensemble-member simulations from 1902 to 1974). Using a two-sided Kolmogorov-Smirnov test, we conclude there is no significant difference ($p \geq 0.05$) in the underlying distributions between either ANZDA series and the CMIP5 ensemble for this interval. (middle column) Number of major drought ($PDSI \leq -1$) and pluvial ($PDSI \geq +1$) years in the ANZDA (tree ring reconstructed and instrumental; green and red dots, respectively) and CMIP5 ensemble (boxplot; 34 different ensemble-member simulations) for the same time interval. (right column) Distributions of drought lengths (years) from the ANZDA (1500–2012) and CMIP5 ensemble (1901–2012), determined using the 2S2E criteria.

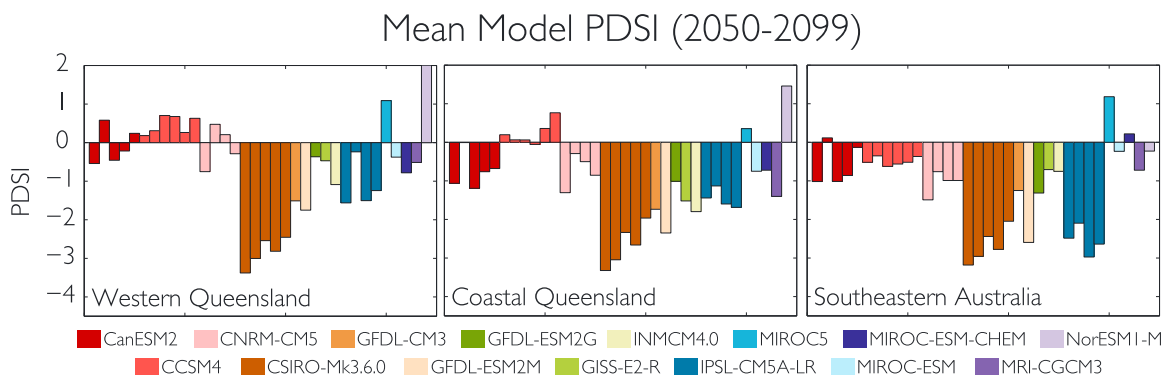


Figure 12. Late 21st century (2050–2099, RCP 8.5 scenario) mean summer (December–January–February; DJF) PDSI for our three regions, calculated from 34 simulations of 15 models in the CMIP5 archive. Each model is represented by a color, and individual bars within a color represent different ensemble-member simulations of the same model (a consequence of different initial conditions). These PDSI projections incorporate model trends in both precipitation and potential evapotranspiration over the 21st century.

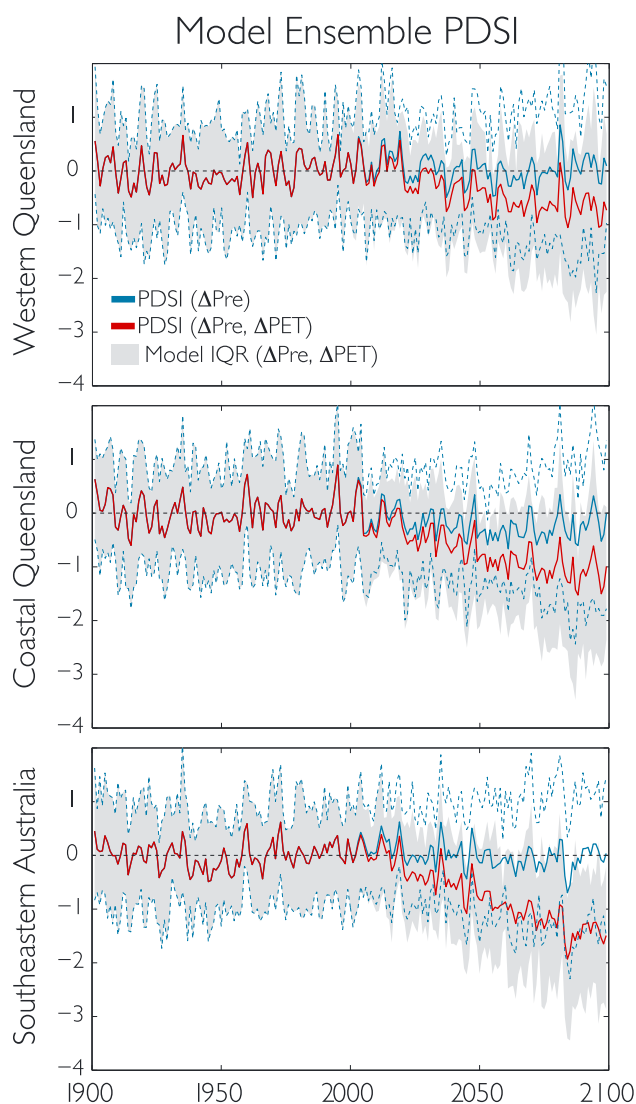


Figure 13. Time series of the ensemble summer (December–January–February; DJF) PDSI (historical+RCP 8.5, 1901–2099) for our three regions, from the same models in Figure 12. The solid blue line is the ensemble average PDSI only incorporating model trends in precipitation, with the associated ensemble spread (cross model interquartile range) shown by the blue dashed lines. The solid red line is the ensemble average PDSI calculated using trends in both precipitation and potential evapotranspiration, with the associated ensemble spread (cross model interquartile range) in the gray shading.

wetting in any region. Among the models in our full ensemble, only three (MIROC-ESM-Chem, MIROC-ESM, and GISS-E2-R) were considered “poor” performers in a recent validation study of the CMIP5 models for Australia [Moise *et al.*, 2015].

To identify the relative contributions of different processes (precipitation or PET) to this drying trend, we calculated alternate versions of the PDSI in which trends in either precipitation or PET over the 21st century were removed. Precipitation-induced declines in PDSI (Figure 13, blue lines) are small in Coastal Queensland (2050–2099, mean PDSI = -0.28) and near zero in Southeastern Australia (PDSI = -0.07) and Western Queensland (PDSI = $+0.01$). Including the effects of changing PET (forced by trends in temperature, humidity, and net radiation) leads to more consistent and substantial drying in all regions (Figure 13, red lines), with the largest amplification in Coastal Queensland (PDSI = -1.00) and Southeastern Australia (PDSI = -1.18). Increases in PET are due primarily to warming-induced increases in the vapor pressure deficit, with secondary contributions from overall increases in surface energy availability. These mechanisms are described in more detail in Cook *et al.* [2014] and other studies [e.g., Scheff and Frierson, 2013].

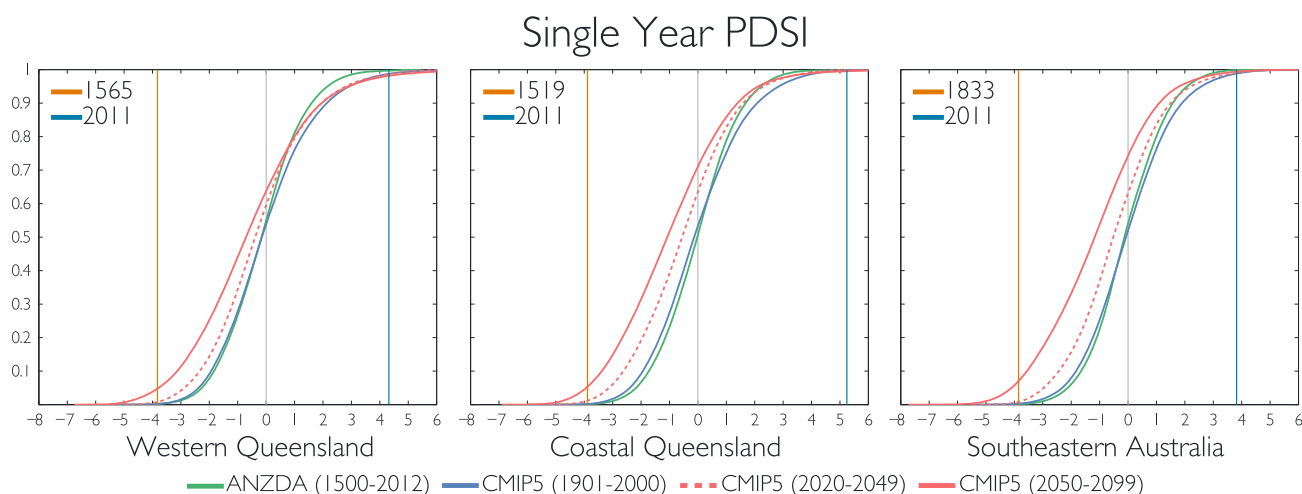


Figure 14. Cumulative kernel density functions for summer (December-January-February; DJF) PDSI, calculated from the ANZDA (1500–2012) and the CMIP5 multimodel ensemble (1901–2000, 2020–2049, and 2050–2099). Vertical lines indicate PDSI values in the ANZDA for 2011 (blue) and the record driest year for each region (brown).

We compared PDSI distributions from the ANZDA (1500–2012) against three intervals from our multimodel ensemble: 1901–2000, 2020–2049, and 2050–2099 (Figure 14). The model distributions incorporate model trends in both precipitation and PET. The progressive drying in the model ensemble from the 20th century to the end of the 21st century is clearly apparent, and, with this drying, the risk of annual PDSI values equal to or drier than the worst drought years in the ANZDA increases substantially. This corresponds to a future risk in different regions of 5% (1565, Western Queensland and 1519, Coastal Queensland) and 7% (1833, Southeastern Australia), well above the baseline estimates (< 1% risk) in the ANZDA. Somewhat paradoxically, the probability of extreme wet years of equal or greater magnitude to 2011 also increases under a scenario of progressive 21st century drying. The likelihood of an extreme event equivalent to or wetter than 2011 increases to 2% (Western Queensland), 0.5% (Coastal Queensland), and 0.6% (Southeastern Australia). While small in absolute terms, the increased risk is relatively large given the exceptionally low likelihood in the ANZDA. An increase in extreme wet years may seem counterintuitive given the mean drying in the PDSI distributions, but this result is generally consistent with the expected response of extreme precipitation and floods to warming [e.g., Easterling et al., 2000; Trenberth, 2011; Trenberth et al., 2015]. This was evident in the 2010–2011 summer, when exceptionally warm SSTs around northern Australia fueled enhanced onshore moisture transport

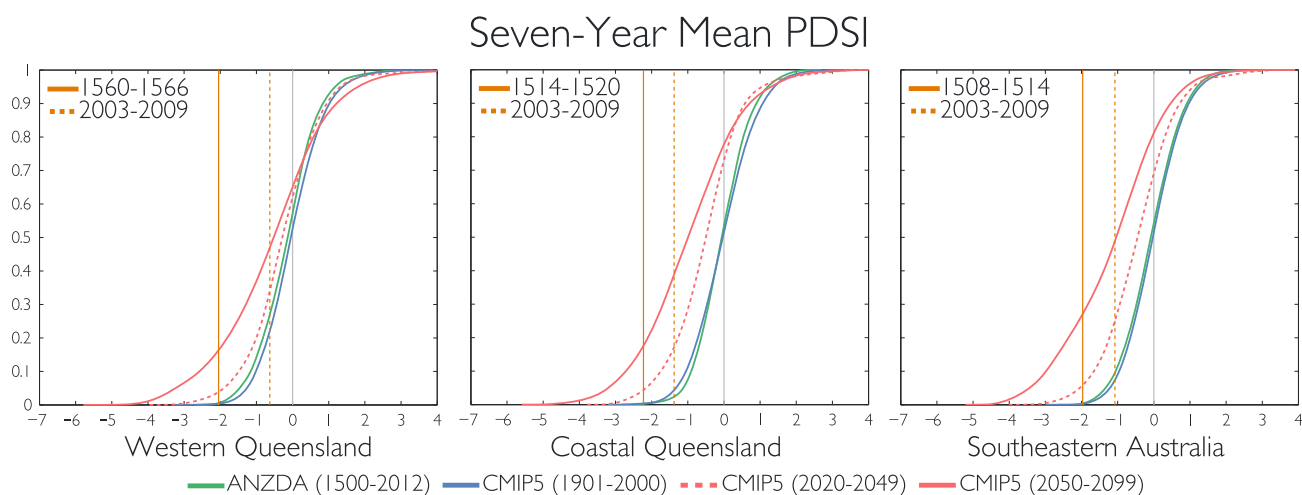


Figure 15. Cumulative kernel density functions for summer (December-January-February; DJF) PDSI calculated on 7-year running mean PDSI. Vertical lines indicate PDSI values for 2003–2009 (Millennium Drought) and the driest 7-year running mean PDSI in each region.

[Evans and Boyer-Souchet, 2012; Ummenhofer et al., 2015]. Even with these increases in likelihood of wet extremes, however, pluvial years analogous to 2011 are likely to remain exceptionally rare.

We conduct a similar analysis in the CMIP5 ensemble for analogues of the Millennium Drought and the driest 7-year running mean in the ANZDA (Figure 15). As with the single year events (Figure 14), the risk of 7-year mean PDSI values equal to or drier than the Millennium Drought increases markedly. For Coastal Queensland and Southeastern Australia, where the Millennium Drought was most strongly expressed, the risk of a similar run of 7-year running mean PDSI values increases from $\leq 10\%$ in the ANZDA to 39% (Coastal Queensland) or 49% (Southeastern Australia) during 2050–2099. Similarly, the risk of 7-year running mean PDSI equal to or drier than the driest 7-year periods increases to $>15\%$ in Western Queensland and Coastal Queensland and $>25\%$ in Southeastern Australia. This indicates that the likelihood of eastern Australia experiencing a 7-year period of summer drought similar to the Millennium Drought increases substantially by the end of the 21st century, under a scenario of continued high levels of greenhouse gas emissions.

4. Discussion and Conclusions

Attribution of climate extremes is a rapidly advancing field of research, especially for hydroclimate events such as floods and droughts [Trenberth et al., 2015]. But one major limitation is the relatively short duration of the instrumental record, which can make it difficult to confidently characterize the full range of natural climate variability. Here we use the ANZDA and projections from the CMIP5 archive to investigate how two recent extreme hydroclimate events in Australia [e.g., Cai et al., 2009b; Evans and Boyer-Souchet, 2012; Hendon et al., 2014; Nicholls, 2004; Ummenhofer et al., 2009, 2015] compare to the last 500 years of natural variability and how their likelihood may shift with increased greenhouse gas forcing.

Neither the single most extreme year of the Millennium Drought (2003) nor the 7-year mean PDSI from 2003 to 2009 appears as unusually severe relative to the last 500 years of natural variability in the ANZDA. Recurrent periods of extreme and persistent drought are apparent in the ANZDA prior to the observational record, consistent with other largely independent reconstructions of hydroclimate for the region [Ho et al., 2015; Vance et al., 2015]. Of note, the ANZDA shows a rather exceptional period of multidecadal drought across eastern Australia in the early 1500s, the most persistent multiyear drought event of the last 500 years. As noted, however, the error estimates in the reconstruction time series are too large to quantitatively and definitively assign ranks for most events. An exception is the extreme pluvial during 2011 over Coastal Queensland, which stands (in terms of summer season PDSI) as nominally the single wettest year in the observational record and reconstruction. This year is a full +1.4 PDSI units wetter than the second wettest year in the reconstruction (1572), and only 12 of the 476 reconstructed years have upper confidence limits exceeding 2011. Viewed probabilistically, this equates to 2011 exceeding 97% of the reconstructed values after taking into account their estimated uncertainties. In light of this result, we conclude that 2011 was likely the wettest summer of the last 500 years in Coastal Queensland, though other years were likely wetter in other parts of Queensland and Southeastern Australia. Comparing against an ensemble of climate projections for the 21st century, average conditions in eastern Australia are expected to become drier in the latter half of the 21st century, with amplified risk of both dry and wet extremes of similar intensity to the Millennium Drought and 2011 pluvial.

Our findings and conclusions regarding these recent events are very likely sensitive to the seasonal precipitation biases in the underlying ANZDA reconstruction. As demonstrated, the summer season PDSI in the ANZDA is most sensitive to summer and antecedent spring precipitation. The ANZDA therefore likely underestimates the severity of the Millennium Drought, which was forced by autumn precipitation deficits that are only weakly and insignificantly expressed in this drought reconstruction. Indeed, independent reconstructions of streamflow [e.g., Gallant and Gergis, 2011] and precipitation [e.g., Gergis et al., 2012] for southeastern Australia confirm the exceptional nature of the Millennium Drought. Conversely, the ANZDA is well suited for evaluation of the 2011 pluvial event, which was forced by extreme summer precipitation.

The PDSI projections in the CMIP5 models have their own set of uncertainties, foremost of which are the structural uncertainties in the models themselves. To address this, we have presented results from each individual model and ensemble member (Figure 12) and used the full multimodel ensemble in our kernel density functions and drought risk analysis. Other studies have criticized PDSI as an overly simplistic drought metric that may overestimate drying trends in response to climate change [e.g., Hoerling et al., 2012; Burke, 2011]. One often-highlighted weakness is the absence of an atmospheric carbon dioxide effect on plant physiology in the standard PDSI calculation, which would be expected to dampen PET-induced drying

[e.g., Roderick *et al.*, 2015]. We consider, however, that PDSI is still a useful and reasonable metric for connecting drought information in the paleoclimate record with model projections. This is supported by the similarities in the 20th century ANZDA and CMIP5 reconstructions (Figure 11), and the general good agreement and comparable trends between PDSI and more complex models of soil moisture for both past and future time intervals found in other studies [Cook *et al.*, 2015; Smerdon *et al.*, 2015; Williams *et al.*, 2015]. Further, there is emerging evidence that the moisture-saving benefits of enhanced carbon dioxide concentrations may be overstated [Frank *et al.*, 2015; Ukkola *et al.*, 2016], especially in land surface and vegetation models [De Kauwe *et al.*, 2013; Kolby Smith *et al.*, 2015]. Finally, we note that the importance of warming and PET as the dominant drying mechanisms in the CMIP5 projections is consistent with recent arguments made for anthropogenic amplification of the Millennium Drought [Cai *et al.*, 2009b; Nicholls, 2004; Ummenhofer *et al.*, 2009].

The Millennium Drought was a prolonged disaster in eastern Australia, with significant agricultural and economic impacts [van Dijk *et al.*, 2013; Heberger, 2011]. Beyond the extreme autumn precipitation deficits, however, the impacts and perception of this drought may have been amplified by other factors. Saft *et al.* [2015], for example, noted that streamflow deficits during the drought were more severe than would have been predicted from precipitation anomalies alone, likely a consequence of climatic and landscape factors. Perceptions may have been further influenced because this drought occurred after an extended period of above-average moisture availability in the decades following the World War II drought. The subsequent period of rapid expansion of agriculture and water resource exploitation in the region may have set unrealistic expectations for moisture availability [Musgrave, 2008]. This was followed by a late 20th century declining trend in autumn rainfall associated with the weather systems most responsible for moisture supply at the start of the winter growing season in southeast Australia [Pook *et al.*, 2009], leading directly into the Millennium Drought. Regardless, the ANZDA suggests that summer-season soil moisture deficits similar to what occurred during the Millennium Drought are not uncommon. These results, therefore, provide strong motivation for policies that will increase resilience given the high likelihood of similar events occurring over the next century from both natural variations and anthropogenic forcing.

Acknowledgments

C.S.M.T. thanks the Australian Research Council for the provision of a Laureate Fellowship. Support was provided by the Australian Research Council through grants FL100100195, and DP130104156 to C.S.M. Turney, LP120100310 to P.F. Grierson, and DP0878744, DP120104320, LP120200811, and FT120100715 for P.J. Baker. B.I. Cook is supported by NASA. The ANZDA is freely available from the NOAA Paleoclimate Archive (<https://www.ncdc.noaa.gov/data-access/paleoclimatology-data/datasets>). Thanks to David Karoly and two anonymous reviewers for providing comments that greatly improved the quality of this manuscript. The authors also thank Linden Ashcroft, for providing the extended precipitation record for Southeastern Australia and additional valuable comments. Lamont contribution 8070.

References

- Allan, R. J. (1985), *The Australasian Summer Monsoon, Teleconnections, and Flooding in the Lake Eyre basin*, R. Geog. Soc. of Australasia, SA Branch.
- Ashcroft, L., D. J. Karoly, and J. Gergis (2014), Southeastern Australian climate variability 1860–2009: A multivariate analysis, *Int. J. Climatol.*, 34(6), 1928–1944, doi:10.1002/joc.3812.
- Australian Bureau of Meteorology (2011), Australian climate variability and change—Time series graphs, website.
- Boening, C., J. K. Willis, F. W. Landerer, R. S. Nerem, and J. Fasullo (2012), The 2011 La Niña: So strong, the oceans fell, *Geophys. Res. Lett.*, 39, L19602, doi:10.1029/2012GL053055.
- Bradstock, R. A. (2010), A biogeographic model of fire regimes in Australia: Current and future implications, *Global Ecol. Biogeogr.*, 19(2), 145–158, doi:10.1111/j.1466-8238.2009.00512.x.
- Burke, E. J. (2011), Understanding the sensitivity of different drought metrics to the drivers of drought under increased atmospheric CO₂, *J. Hydrometeorol.*, 12(6), 1378–1394, doi:10.1175/2011JHM1386.1.
- Cai, W., and P. van Rensch (2012), The 2011 southeast Queensland extreme summer rainfall: A confirmation of a negative Pacific Decadal Oscillation phase?, *Geophys. Res. Lett.*, 39, L08702, doi:10.1029/2011GL050820.
- Cai, W., T. Cowan, and M. Raupach (2009a), Positive Indian Ocean Dipole events precondition southeast Australia bushfires, *Geophys. Res. Lett.*, 36, L19710, doi:10.1029/2009GL039902.
- Cai, W., T. Cowan, P. Briggs, and M. Raupach (2009b), Rising temperature depletes soil moisture and exacerbates severe drought conditions across southeast Australia, *Geophys. Res. Lett.*, 36, L21709, doi:10.1029/2009GL040334.
- Cai, W., P. van Rensch, T. Cowan, and A. Sullivan (2010), Asymmetry in ENSO teleconnection with regional rainfall, its multidecadal variability, and impact, *J. Clim.*, 23(18), 4944–4955.
- Cai, W., P. van Rensch, T. Cowan, and H. H. Hendon (2011), Teleconnection pathways of ENSO and the IOD and the mechanisms for impacts on Australian rainfall, *J. Clim.*, 24(15), 3910–3923, doi:10.1175/2011JCLI4129.1.
- Cai, W., A. Purich, T. Cowan, P. van Rensch, and E. Weller (2014), Did climate change-induced rainfall trends contribute to the Australian millennium drought?, *J. Clim.*, 27(9), 3145–3168, doi:10.1175/JCLI-D-13-00322.1.
- Coats, S., J. E. Smerdon, R. Seager, B. I. Cook, and J. F. González-Rouco (2013), Megadroughts in southwestern North America in ECHO-G millennial simulations and their comparison to proxy drought reconstructions, *J. Clim.*, 26(19), 7635–7649, doi:10.1175/JCLI-D-12-00603.1.
- Coats, S., J. E. Smerdon, B. I. Cook, and R. Seager (2015), Are simulated megadroughts in the North American southwest forced?, *J. Clim.*, 28(1), 124–142, doi:10.1175/JCLI-D-14-00071.1.
- Cook, B. I., J. E. Smerdon, R. Seager, and S. Coats (2014), Global warming and 21st century drying, *Clim. Dyn.*, 43(9–10), 2607–2627, doi:10.1007/s00382-014-2075-y.
- Cook, B. I., T. R. Ault, and J. E. Smerdon (2015), Unprecedented 21st century drought risk in the American Southwest and Central Plains, *Sci. Adv.*, 1(1), 1400082, doi:10.1126/sciadv.1400082.
- Cook, E. R., C. A. Woodhouse, C. M. Eakin, D. M. Meko, and D. W. Stahle (2004), Long-term aridity changes in the western United States, *Science*, 306(5698), 1015–1018, doi:10.1126/science.1102586.
- Cook, E. R., K. J. Anchukaitis, B. M. Buckley, R. D. D'Arrigo, G. C. Jacoby, and W. E. Wright (2010), Asian monsoon failure and megadrought during the last millennium, *Science*, 328(5977), 486–489, doi:10.1126/science.1185188.

- Cullen, L. E., and P. F. Grierson (2009), Multi-decadal scale variability in autumn-winter rainfall in south-western Australia since 1655 AD as reconstructed from tree rings of *Callitris columellaris*, *Clim. Dyn.*, 33(2), 433–444, doi:10.1007/s00382-008-0457-8.
- De Kauwe, M. G., et al. (2013), Forest water use and water use efficiency at elevated CO₂: A model-data intercomparison at two contrasting temperate forest FACE sites, *Global Change Biol.*, 19(6), 1759–1779, doi:10.1111/gcb.12164.
- Easterling, D., J. Evans, P. Groisman, T. Karl, K. Kunkel, and P. Ambenje (2000), Observed variability and trends in extreme climate events: A brief review, *Bull. Am. Meteorol. Soc.*, 81(3), 417–425.
- Evans, J. P., and I. Boyer-Souchet (2012), Local sea surface temperatures add to extreme precipitation in northeast Australia during La Niña, *Geophys. Res. Lett.*, 39, L10803, doi:10.1029/2012GL052014.
- Fasullo, J. T., C. Boening, F. W. Landerer, and R. S. Nerem (2013), Australia's unique influence on global sea level in 2010–2011, *Geophys. Res. Lett.*, 40, 4368–4373, doi:10.1002/grl.50834.
- Frank, D. C., et al. (2015), Water-use efficiency and transpiration across European forests during the Anthropocene, *Nat. Clim. Change*, 5(6), 579–583, doi:10.1038/nclimate2614.
- Gallant, A. J. E., and J. Gergis (2011), An experimental streamflow reconstruction for the River Murray, Australia, 1783–1988, *Water Resour. Res.*, 47, W00G04, doi:10.1029/2010WR009832.
- Gergis, J., and L. Ashcroft (2013), Rainfall variations in south-eastern Australia part 2: A comparison of documentary, early instrumental and palaeoclimate records, 1788–2008, *Int. J. Climatol.*, 33(14), 2973–2987, doi:10.1002/joc.3639.
- Gergis, J., A. Gallant, K. Braganza, D. Karoly, K. Allen, L. Cullen, R. D'Arrigo, I. Goodwin, P. Grierson, and S. McGregor (2012), On the long-term context of the 1997–2009 'Big Dry' in South-Eastern Australia: Insights from a 206-year multi-proxy rainfall reconstruction, *Clim. Change*, 111(3–4), 923–944, doi:10.1007/s10584-011-0263-x.
- Grove, R. H. (1998), Global impact of the 1789–93 El Niño, *Nature*, 393(6683), 318–319, doi:10.1038/30636.
- Guttman, N. B. (1998), Comparing the Palmer drought index and the standardized precipitation index, *J. Am. Water Resour. Assoc.*, 34, 113–121, doi:10.1111/j.1752-1688.1998.tb05964.x.
- Harris, I., P. D. Jones, T. J. Osborn, and D. H. Lister (2014), Updated high-resolution grids of monthly climatic observations—The CRU TS3.10 dataset, *Int. J. Climatol.*, 34(3), 623–642, doi:10.1002/joc.3711.
- Heberger, M. (2011), Australia's millennium drought: Impacts and responses, in *The World's Water*, edited by P. H. Gleick, pp. 97–125, Island Press/Cent. for Resour. Econ., Washington, D. C., doi:10.5822/978-1-59726-228-6_5.
- Hendon, H. H., E.-P. Lim, J. M. Arblaster, and D. L. T. Anderson (2014), Causes and predictability of the record wet east Australian spring 2010, *Clim. Dyn.*, 42(5–6), 1155–1174, doi:10.1007/s00382-013-1700-5.
- Ho, M., A. S. Kiem, and D. C. Verdon-Kidd (2015), A paleoclimate rainfall reconstruction in the Murray-Darling Basin (MDB), Australia: 2. Assessing hydroclimatic risk using paleoclimate records of wet and dry epochs, *Water Resour. Res.*, 51, 8380–8396, doi:10.1002/2015WR017059.
- Hoerling, M. P., J. K. Eischeid, X.-W. Quan, H. F. Diaz, R. S. Webb, R. M. Dole, and D. R. Easterling (2012), Is a transition to semipermanent drought conditions imminent in the U.S. Great Plains?, *J. Clim.*, 25(24), 8380–8386, doi:10.1175/JCLI-D-12-00449.1.
- Holmes, C. E. (2012), *Queensland Floods Commission of Inquiry: Final Report*, Queensland Floods Commission of Inquiry.
- Horridge, M., J. Madden, and G. Wittwer (2005), The impact of the 2002–2003 drought on Australia, *J. Policy Model.*, 27(3), 285–308, doi:10.1016/j.jpolmod.2005.01.008, world Economy and European Integration.
- Kiem, A. S., and S. W. Franks (2004), Multi-decadal variability of drought risk, eastern Australia, *Hydrol. Processes*, 18(11), 2039–2050, doi:10.1002/hyp.1460.
- Kiem, A. S., and D. C. Verdon-Kidd (2010), Towards understanding hydroclimatic change in Victoria, Australia—Preliminary insights into the "Big Dry", *Hydrol. Earth Syst. Sci.*, 14(3), 433–445, doi:10.5194/hess-14-433-2010.
- Kiem, A. S., S. W. Franks, and G. Kuczera (2003), Multi-decadal variability of flood risk, *Geophys. Res. Lett.*, 30(2), 1035, doi:10.1029/2002GL015992.
- Kirby, M., R. Bark, J. Connor, M. E. Qureshi, and S. Keyworth (2014), Sustainable irrigation: How did irrigated agriculture in Australia's Murray–Darling Basin adapt in the Millennium Drought?, *Agric. Water Manage.*, 145, 154–162, doi:10.1016/j.agwat.2014.02.013, exploring some of the socio-economic realities of sustainable water management in irrigation.
- Kolby Smith, W., S. C. Reed, C. C. Cleveland, A. P. Ballantyne, W. R. L. Anderegg, W. R. Wieder, Y. Y. Liu, and S. W. Running (2015), Large divergence of satellite and Earth system model estimates of global terrestrial CO₂ fertilization, *Nature Clim. Change*, 6, 306–310, doi:10.1038/nclimate2879, advance online publication.
- Le Quéré, C., et al. (2013), The global carbon budget 1959–2011, *Earth Syst. Sci. Data*, 5(1), 165–185, doi:10.5194/essd-5-165-2013.
- Lewis, S. C., and D. J. Karoly (2015), Are estimates of anthropogenic and natural influences on Australia's extreme 2010–2012 rainfall model-dependent?, *Clim. Dyn.*, 45(3–4), 679–695.
- Li, J., et al. (2013), El Niño modulations over the past seven centuries, *Nat. Clim. Change*, 3(9), 822–826, doi:10.1038/nclimate1936.
- Lockart, N., D. Kavetski, and S. W. Franks (2009), On the recent warming in the Murray-Darling Basin: Land surface interactions misunderstood, *Geophys. Res. Lett.*, 36, L24405, doi:10.1029/2009GL040598.
- Moise, A., et al. (2015), Evaluation of CMIP3 and CMIP5 models over the Australian region to inform confidence in projections, *Aust. Meteorol. Oceanogr. J.*, 65(1), 19–53.
- Musgrave, W. (2008), Historical development of water resources in Australia: Irrigation policy in the Murray-Darling Basin, in *Water Policy in Australia: The Impact of Change and Uncertainty*, edited by L. Crase, pp. 28–43, Resour. for the Future, Washington, D. C.
- Nicholls, N. (2004), The changing nature of Australian droughts, *Clim. Change*, 63(3), 323–336, doi:10.1023/B:CLIM.0000018515.46344.6d.
- Nicholls, N., B. Lavery, C. Frederiksen, W. Drosowsky, and S. Torok (1996), Recent apparent changes in relationships between the El Niño–Southern Oscillation and Australian rainfall and temperature, *Geophys. Res. Lett.*, 23(23), 3357–3360, doi:10.1029/96GL03166.
- Palmer, J. G., E. R. Cook, C. S. M. Turney, K. Allen, P. Fenwick, B. I. Cook, A. O'Donnell, J. Lough, P. Grierson, and P. Baker (2015), Drought variability in the eastern Australia and New Zealand summer drought atlas (ANZDA, CE 1500–2012) modulated by the Interdecadal Pacific Oscillation, *Environ. Res. Lett.*, 10(12), 124002, doi:10.1088/1748-9326/10/12/124002.
- Palmer, W. C. (1965), Meteorological drought, Tech. Rep., US Weather Bureau, Washington, D. C.
- Pittock, B., D. Abbs, R. Suppiah, and R. Jones (2006), Climatic background to past and future floods in Australia, *Adv. Ecol. Res.*, 39, 13–39, doi:10.1016/S0065-2504(06)39002-2.
- Pook, M., S. Lisson, J. Risbey, C. C. Ummenhofer, P. McIntosh, and M. Rebbeck (2009), The autumn break for cropping in southeast Australia: Trends, synoptic influences and impacts on wheat yield, *Int. J. Climatol.*, 29(13), 2012–2026, doi:10.1002/joc.1833.
- Pook, M. J., P. C. McIntosh, and G. A. Meyers (2006), The synoptic decomposition of cool-season rainfall in the southeastern Australian cropping region, *J. Appl. Meteorol. Climatol.*, 45(8), 1156–1170, doi:10.1175/JAM2394.1.
- Post, D. A., B. Timbal, F. H. S. Chiew, H. H. Hendon, H. Nguyen, and R. Moran (2014), Decrease in southeastern Australian water availability linked to ongoing Hadley cell expansion, *Earth's Future*, 2(4), 231–238, doi:10.1002/2013EF000194.

- Potter, N. J., F. H. S. Chiew, and A. J. Frost (2010), An assessment of the severity of recent reductions in rainfall and runoff in the Murray–Darling Basin, *J. Hydrol.*, *381*(1–2), 52–64, doi:10.1016/j.jhydrol.2009.11.025.
- Poulter, B., et al. (2014), Contribution of semi-arid ecosystems to interannual variability of the global carbon cycle, *Nature*, *509*(7502), 600–603, doi:10.1038/nature13376.
- Power, S., F. Tseitin, S. Torok, B. Lavery, R. Dahni, and B. McAvaney (1998), Australian temperature, Australian rainfall and the Southern Oscillation, 1910–1992: Coherent variability and recent changes, *Aust. Meteorol. Mag.*, *47*(2), 85–101.
- Power, S., T. Casey, C. Folland, A. Colman, and V. Mehta (1999), Inter-decadal modulation of the impact of ENSO on Australia, *Clim. Dyn.*, *15*(5), 319–324, doi:10.1007/s003820050284.
- Quiggin, J. (2001), Environmental economics and the Murray–Darling river system, *Aust. J. Agr. Resour. Econ.*, *45*(1), 67–94, doi:10.1111/1467-8489.00134.
- Risbey, J. S., M. J. Pook, P. C. McIntosh, M. C. Wheeler, and H. H. Hendon (2009), On the remote drivers of rainfall variability in Australia, *Mon. Weather Rev.*, *137*(10), 3233–3253, doi:10.1175/2009MWR2861.1.
- Roderick, M. L., P. Greve, and G. D. Farquhar (2015), On the assessment of aridity with changes in atmospheric CO₂, *Water Resour. Res.*, *51*, 5450–5463, doi:10.1002/2015WR017031.
- Russell, H. C. (1877), *Climate of New South Wales: Descriptive, Historical, and Tabular*, C. Potter for Gov. Print., 252 pp., Sydney, Australia.
- Saft, M., A. W. Western, L. Zhang, M. C. Peel, and N. J. Potter (2015), The influence of multiyear drought on the annual rainfall-runoff relationship: An Australian perspective, *Water Resour. Res.*, *51*, 2444–2463, doi:10.1002/2014WR015348.
- Scheff, J., and D. M. W. Frierson (2013), Scaling potential evapotranspiration with greenhouse warming, *J. Clim.*, *27*, 1539–1558, doi:10.1175/JCLI-D-13-00233.1.
- Smerdon, J. E., B. I. Cook, E. R. Cook, and R. Seager (2015), Bridging past and future climate across paleoclimatic reconstructions, observations, and models: hydroclimate case study, *J. Clim.*, *28*(8), 3212–3231, doi:10.1175/JCLI-D-14-00417.1.
- Taylor, K. E., R. J. Stouffer, and G. A. Meehl (2012), An overview of CMIP5 and the experiment design, *Bull. Am. Meteorol. Soc.*, *93*(4), 485–498, doi:10.1175/BAMS-D-11-00094.1.
- Teague, B., R. McLeod, and S. Pascoe (2010), Final report summary of the 2009 Victorian Bushfires Royal Commission, *Tech. Rep.*, Government Printer for the State of Victoria, Victoria.
- Theobald, A., H. McGowan, and J. Speirs (2015), Trends in synoptic circulation and precipitation in the Snowy Mountains region, Australia, in the period 1958–2012, *Atmos. Res.*, *169*, 434–448, doi:10.1016/j.atmosres.2015.05.007.
- Timbal, B., and R. Fawcett (2012), A historical perspective on southeastern Australian rainfall since 1865 using the instrumental record, *J. Clim.*, *26*(4), 1112–1129, doi:10.1175/JCLI-D-12-00082.1.
- Timbal, B., and R. Fawcett (2013), A historical perspective on southeastern Australian rainfall since 1865 using the instrumental record, *J. Clim.*, *26*(4), 1112–1129, doi:10.1175/JCLI-D-12-00082.1.
- Trenberth, K. E. (2011), Changes in precipitation with climate change, *Clim. Res.*, *47*(1), 123–138, doi:10.3354/cr00953.
- Trenberth, K. E., J. T. Fasullo, and T. G. Shepherd (2015), Attribution of climate extreme events, *Nat. Clim. Change*, *5*(8), 725–730, doi:10.1038/nclimate2657.
- Ukkola, A. M., I. C. Prentice, T. F. Keenan, A. I. J. M. van Dijk, N. R. Viney, R. B. Myneni, and J. Bi (2016), Reduced streamflow in water-stressed climates consistent with CO₂ effects on vegetation, *Nat. Clim. Change*, *6*(1), 75–78, doi:10.1038/nclimate2831.
- Ummenhofer, C. C., M. H. England, P. C. McIntosh, G. A. Meyers, M. J. Pook, J. S. Risbey, A. S. Gupta, and A. S. Taschetto (2009), What causes southeast Australia's worst droughts?, *Geophys. Res. Lett.*, *36*, L04706, doi:10.1029/2008GL036801.
- Ummenhofer, C. C., A. Sen Gupta, P. R. Briggs, M. H. England, P. C. McIntosh, G. A. Meyers, M. J. Pook, M. R. Raupach, and J. S. Risbey (2011), Indian and Pacific Ocean influences on southeast Australian drought and soil moisture, *J. Clim.*, *24*(5), 1313–1336, doi:10.1175/2010JCLI3475.1.
- Ummenhofer, C. C., A. Sen Gupta, M. H. England, A. S. Taschetto, P. R. Briggs, and M. R. Raupach (2015), How did ocean warming affect Australian rainfall extremes during the 2010/2011 La Niña event?, *Geophys. Res. Lett.*, *42*, 9942–9951, doi:10.1002/2015GL063948.
- van den Honert, R. C., and J. McAneney (2011), The 2011 Brisbane floods: Causes, impacts and implications, *Water*, *3*(4), 1149, doi:10.3390/w3041149.
- van der Schrier, G., J. Barichivich, K. R. Briffa, and P. D. Jones (2013), A scPDSI-based global data set of dry and wet spells for 1901–2009, *J. Geophys. Res. Atmos.*, *118*, 4025–4048, doi:10.1002/jgrd.50355.
- van Dijk, A. I. J. M., H. E. Beck, R. S. Crosbie, R. A. M. de Jeu, Y. Y. Liu, G. M. Podger, B. Timbal, and N. R. Viney (2013), The Millennium Drought in southeast Australia (2001–2009): Natural and human causes and implications for water resources, ecosystems, economy, and society, *Water Resour. Res.*, *49*, 1040–1057, doi:10.1002/wrcr.20123.
- Vance, T. R., J. L. Roberts, C. T. Plummer, A. S. Kiem, and T. D. van Ommen (2015), Interdecadal Pacific variability and eastern Australian megadroughts over the last millennium, *Geophys. Res. Lett.*, *42*, 129–137, doi:10.1002/2014GL062447.
- Verdon-Kidd, D. C., and A. S. Kiem (2009), Nature and causes of protracted droughts in southeast Australia: Comparison between the Federation, WWII, and Big Dry droughts, *Geophys. Res. Lett.*, *36*, L22707, doi:10.1029/2009GL041067.
- Verdon-Kidd, D. C., A. S. Kiem, and R. Moran (2014), Links between the Big Dry in Australia and hemispheric multi-decadal climate variability—Implications for water resource management, *Hydrol. Earth Syst. Sci.*, *18*(6), 2235–2256, doi:10.5194/hess-18-2235-2014.
- Wei, Y., J. Langford, I. R. Willett, S. Barlow, and C. Lyle (2011), Is irrigated agriculture in the Murray–Darling Basin well prepared to deal with reductions in water availability?, *Global Environ. Change*, *21*(3), 906–916, doi:10.1016/j.gloenvcha.2011.04.004, symposium on Social Theory and the Environment in the New World (dis)Order.
- Williams, A. P., R. Seager, J. T. Abatzoglou, B. I. Cook, J. E. Smerdon, and E. R. Cook (2015), Contribution of anthropogenic warming to the 2012–2014 California drought, *Geophys. Res. Lett.*, *42*, 6819–6828, doi:10.1002/2015GL064924.
- Young, M. D., and J. C. McColl (2003), Robust reform: The case for a new water entitlement system for Australia, *Aust. Econ. Rev.*, *36*(2), 225–234, doi:10.1111/1467-8462.00282.